SEMI-BLIND CHANNEL ESTIMATION FOR OFDM-BASED AMPLIFY-AND-FORWARD TWO-WAY RELAY NETWORKS

Saeed Abdallah and Ioannis N. Psaromiligkos

McGill University, Department of Electrical & Computer Engineering
Montreal, Quebec, Canada, H3A 2A7
Email: saeed.abdallah@mail.mcgill.ca, ioannis.psaromiligkos@mcgill.ca

ABSTRACT

We consider the problem of channel estimation for OFDM-based amplify-and-forward (AF) two-way relay networks (TWRNs). Unlike previous works which were based on a fully pilot-based approach, we propose a semi-blind approach that exploits both the transmitted pilots as well as the received data samples to provide an enhanced estimation performance. Superimposed training is adopted at the relay to assist in the estimation of the individual channels. We base our semi-blind estimator on the maximum-likelihood (ML) criterion and employ an iterative low-complexity Quasi-Newton method to obtain the ML semi-blind channel estimates. As a performance benchmark we derive the semi-blind Cramer-Rao bound (CRB). Using simulation studies, we show that the proposed approach provides a substantial improvement in estimation accuracy over the conventional pilot-based approach.

Index Terms— Amplify-and-forward relays, OFDM, semi-blind channel estimation, superimposed training, two-way relays.

1. INTRODUCTION

Two-way relay networks [1] (TWRNs) have attracted the attention of many researchers as a spectrally efficient solution for bidirectional communication. In studying TWRNs, researchers have considered both the amplify-and-forward (AF) and the decode-and-forward (DF) relaying protocols. AF TWRNs are appealing due to the minimal processing they require at the relay. However, they require highly accurate information about the channel to cancel the inherent self-interference at the terminals. Hence, it is essential to develop accurate and efficient channel estimation algorithms for AF TWRNs.

The problem of channel estimation for AF TWRNs has been studied in several recent works [2–7]. Some of these assume flat-fading channel conditions [2–4], while others [5–7] consider the more challenging case of frequency selective fading where OFDM transmission is employed to combat the multipath phenomenon. In both cases, most previous works adopt a fully pilot-based approach that estimates the channel parameters exclusively through the use of pilot symbols [3–7]. This approach does not exploit the known self-interference symbols present in the received signals at each terminal during data transmission, that can serve as pseudo-pilots to improve the estimation performance. To capitalize on the presence of these pseudo-pilots, blind and semi-blind estimation techniques can be employed. Blind estimation relies only on the data samples to estimate the channels, but the use of a small number of pilots is still needed to resolve inherent ambiguity. Assuming flat-fading conditions, blind estimation was used to estimate the cascaded (composite) channels for MPSK-based AF TWRNs in [2]. For the frequency-selective scenario, an algorithm was developed in [8] to estimate the cascaded channels blindly using the second-order statistics of the received signal. As shown in [8], a large number of OFDM symbols is required to achieve accurate channel estimation blindly in the frequency-selective environment. The semi-blind approach, on the other hand, is more flexible as it incorporates into the estimation both the pilots as well as the received data samples. For the estimation of cascaded channels under flat-fading conditions, it was shown in [9] that the semi-blind approach provides substantially higher accuracy than the pilot-based approach while employing only a limited number of data samples and the same number of pilots as the pilot-based approach. For MIMO-OFDM based AF TWRNs, a semi-blind algorithm was proposed in [10] to jointly estimate the cascaded channels and decode the data using the expectation conditional maximization approach with soft interference cancellation.

In this work, we consider semi-blind channel estimation for OFDM-based AF TWRNs. As done in [5–7], we focus on the estimation of the individual channels, rather than the cascaded channels. Although the cascaded channels are sufficient for detection, the individual channels are useful in their own right as they are often needed in other applications such as beamforming [11]. To assist in the estimation of the individual channels, we adopt a superimposed training strategy at the relay. This strategy has been applied before in the context of pilot-based estimation [7, 12], but we are the first to use it for semi-blind estimation in AF TWRNs, to the best of our knowledge. Our proposed estimator is based on the maximum-likelihood (ML) criterion. To simplify the semi-blind likelihood function, the transmitted data is assumed to be Gaussian distributed. The ML channel estimates are obtained numerically using an iterative Quasi-Newton method. As a benchmark on estimation performance, we also derive the semi-blind Cramer-Rao bound (CRB). Using simulations, we show that the proposed semi-blind estimator closely approaches the semi-blind CRB and provides substantial improvements in accuracy over the pilot-based approach, even when the data symbols are drawn from discrete constellations, e.g., QPSK.

The rest of the paper is organized as follows. In Section 2 we present the system model. The proposed semi-blind channel estimation algorithm is presented in Section 3. The CRBs are derived in Section 4. Simulation results are presented in Section 5. Finally, our conclusions are in Section 6.

This work was supported in part by the Natural Sciences and Engineering Research Council (NSERC).

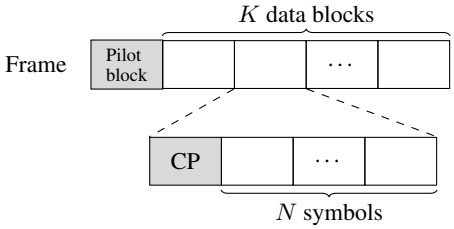

Fig. 1. Structure of the OFDM frame transmitted by the terminals.

2. SYSTEM MODEL

We consider a half-duplex AF TWRN with two source nodes, $\mathcal{T}_1$ and $\mathcal{T}_2$, and a single relaying node $\mathcal{R}$ which operates in frequency selective channel conditions. To compensate for the multipath phenomenon, OFDM transmission is employed, using N subcarriers. Data is exchanged between $\mathcal{T}_1$ and $\mathcal{T}_2$ in rounds that consist of two phases. In the first phase, the two terminals simultaneously transmit an OFDM frame to $\mathcal{R}$. In the second phase, $\mathcal{R}$ broadcasts an amplified version of the received frame.

2.1. Transmission at the Terminals

Each OFDM frame transmitted by the terminals is composed of one pilot block and K data blocks (see Fig. 1). Furthermore, each OFDM block (pilot or data) consists of N time-domain symbols and a cyclic prefix (CP) of appropriate length that is inserted to avoid inter-block interference. We denote by $\tilde{\boldsymbol{t}}_1$ and $\tilde{\boldsymbol{t}}_2$ the $N\times 1$ frequency-domain pilot symbol vectors of $\mathcal{T}_1$ and $\mathcal{T}_2$, and by $\tilde{\boldsymbol{s}}_{1k}$ and $\tilde{\boldsymbol{s}}_{2k}$, $k=1,\ldots,K$, the $N\times 1$ frequency-domain data symbol vectors of $\mathcal{T}_1$ and $\mathcal{T}_2$, respectively. The corresponding time-domain pilot and data symbol vectors are $\boldsymbol{t}_1 = \boldsymbol{F}^H\tilde{\boldsymbol{t}}_1$, $\boldsymbol{t}_2 = \boldsymbol{F}^H\tilde{\boldsymbol{t}}_2$, $\boldsymbol{s}_{1k} = \boldsymbol{F}^H\tilde{\boldsymbol{s}}_{1k}$ and $\boldsymbol{s}_{2k} = \boldsymbol{F}^H\tilde{\boldsymbol{s}}_{2k}$, $k=1,\ldots,K$, where $\boldsymbol{F}$ is the $N\times N$ normalized discrete Fourier transform (DFT) matrix whose (p,q)th entry is $1/\sqrt{N}e^{-\jmath 2\pi(p-1)(q-1)/N}$. Moreover, we assume that the average transmission powers of $\mathcal{T}_1$ and $\mathcal{T}_2$ during pilot transmission are P_1 and P_2, respectively, i.e., $\tilde{\boldsymbol{t}}_1^H\tilde{\boldsymbol{t}}_1 = NP_1$ and $\tilde{\boldsymbol{t}}_2^H\tilde{\boldsymbol{t}}_2 = NP_2$. For simplicity, we also assume that the same average transmission powers are employed by the terminals for data transmission, that is, $\mathbb{E}\left\{\boldsymbol{s}_{1k}^H\boldsymbol{s}_{1k}\right\} = NP_1$ and $\mathbb{E}\left\{\boldsymbol{s}_{2k}^H\boldsymbol{s}_{2k}\right\} = NP_2$.

The baseband channels from $\mathcal{T}_1$ to $\mathcal{R}$ and from $\mathcal{T}_2$ to $\mathcal{R}$ are denoted by $\boldsymbol{h} \triangleq [h_1,\ldots,h_L]^T$, and $\boldsymbol{g} \triangleq [g_1,\ldots,g_J]^T$, respectively. The elements of $\boldsymbol{h}$ and $\boldsymbol{g}$ are modelled as independent and identically distributed (i.i.d.) circular complex Gaussian random variables with mean zero and variance γ^2. We also assume quasi-static channel conditions, such that the channels $\boldsymbol{h}$ and $\boldsymbol{g}$ are fixed for the frame duration.

2.2. Processing at the Relay

The received vector at the relay corresponding to the transmitted pilot blocks after CP removal is given by

$$\boldsymbol{r} = \boldsymbol{H}\boldsymbol{t}_1 + \boldsymbol{G}\boldsymbol{t}_2 + \boldsymbol{n}, \tag{1}$$

where $\boldsymbol{H}$ and $\boldsymbol{G}$ are $N\times N$ circulant matrices with first columns $[\boldsymbol{h}^T,\boldsymbol{0}_{1\times(N-L)}]^T$ and $[\boldsymbol{g}^T,\boldsymbol{0}_{1\times(N-J)}]^T$, respectively, and $\boldsymbol{n}$ is circular complex white Gaussian noise vectors with mean zero and covariance[1] $\sigma^2\boldsymbol{I}_N$, denoted as $\mathcal{CCN}(0,\sigma^2\boldsymbol{I}_N)$. Similarly, the received vectors corresponding to the K data blocks are

$$\boldsymbol{r}_k = \boldsymbol{H}\boldsymbol{s}_{1k} + \boldsymbol{G}\boldsymbol{s}_{2k} + \boldsymbol{n}_k, \tag{2}$$

where $\boldsymbol{n}_1,\ldots,\boldsymbol{n}_K$ are also $\mathcal{CCN}(0,\sigma^2\boldsymbol{I}_N)$.

The relay first amplifies the received pilot block, using an amplification factor $A_p > 0$. Then, to assist channel estimation at the terminals, it superimposes[2] [7] over the amplified vector $A_p\boldsymbol{r}$ a time-domain pilot vector $\boldsymbol{t}_3 = \boldsymbol{F}^H\tilde{\boldsymbol{t}}_3$, where $\tilde{\boldsymbol{t}}_3$ is the corresponding frequency-domain vector. The resulting signal vector is given by

$$A_p\boldsymbol{r} + \boldsymbol{t}_3 = A_p\boldsymbol{H}\boldsymbol{t}_1 + A_p\boldsymbol{G}\boldsymbol{t}_2 + A_p\boldsymbol{n} + \boldsymbol{t}_3. \tag{3}$$

The average transmission power of the relay over the long term (i.e., over many OFDM frames) is set at P_r. This power is divided between the amplified signal vector $A_p\boldsymbol{r}$ and the superimposed vector $\boldsymbol{t}_3$. More specifically, αP_r is allocated to the superimposed pilot and $(1-\alpha)P_r$ is allocated to $A_p\boldsymbol{r}$, where $0<\alpha<1$. Using the statistics of the channels $\boldsymbol{h}$ and $\boldsymbol{g}$, it can be shown that $N^{-1}\mathbb{E}\{\boldsymbol{r}^H\boldsymbol{r}\} = L\gamma^2P_1 + J\gamma^2P_2 + \sigma^2$. Hence, to allocate $(1-\alpha)P_r$ to the amplified signal, the amplification factor should be set as $A_p = \sqrt{\frac{(1-\alpha)P_r}{L\gamma^2P_1+J\gamma^2P_2+\sigma^2}}$.

The relay also amplifies the information-bearing vectors $\boldsymbol{r}_k$, using an amplification factor $A_d > 0$, but without superimposing a pilot. In this case, the relay can maintain an average transmission power of P_r by using $A_d = \sqrt{\frac{P_r}{L_1\gamma^2P_1+J_1\gamma^2P_2+\sigma^2}}$. Before broadcasting the frame that contains the amplified pilot and data vectors, the relay inserts a new CP into each block in the frame.

2.3. Received Vectors at the Terminal

Assuming reciprocal channels, the pilot-bearing received signal block at $\mathcal{T}_1$ after CP removal is given by

$$\boldsymbol{y} = A_p\boldsymbol{H}\boldsymbol{H}\boldsymbol{t}_1 + A_p\boldsymbol{H}\boldsymbol{G}\boldsymbol{t}_2 + \boldsymbol{H}\boldsymbol{t}_3 + A_p\boldsymbol{H}_2\boldsymbol{n} + \boldsymbol{w}. \tag{4}$$

Moreover, the K information bearing received signal blocks are given by

$$\boldsymbol{z}_k = A_d\boldsymbol{H}\boldsymbol{H}\boldsymbol{s}_{1k} + A_d\boldsymbol{H}\boldsymbol{G}\boldsymbol{s}_{2k} + A_d\boldsymbol{H}\boldsymbol{n}_k + \boldsymbol{w}_k, \tag{5}$$

where $\boldsymbol{w}_1,\ldots,\boldsymbol{w}_K$ are also $\mathcal{CCN}(0,\sigma^2\boldsymbol{I}_N)$.

3. SEMI-BLIND CHANNEL ESTIMATION

In this section, we present the proposed semi-blind channel estimation algorithm. The channel parameters are collected into the vector $\boldsymbol{\theta} \triangleq [\boldsymbol{h}^T,\boldsymbol{g}^T]^T$. To derive the semi-blind estimator, we will use the joint likelihood function of the vectors $\boldsymbol{y},\boldsymbol{z}_1,\ldots,\boldsymbol{z}_K$. This likelihood function depends on the specific constellation from which the frequency-domain data symbol vectors $\tilde{\boldsymbol{s}}_{21},\ldots,\tilde{\boldsymbol{s}}_{2K}$ are drawn. Unfortunately, taking into account the discrete statistics of these vectors would result in a very complicated likelihood function. Instead, we obtain a more tractable function by resorting to the Gaussian approximation and modelling the data vectors $\tilde{\boldsymbol{s}}_{21},\ldots,\tilde{\boldsymbol{s}}_{2K}$ as i.i.d.

[1] $\boldsymbol{I}_N$ denotes the $N\times N$ identity matrix.

[2] The superimposed pilot makes the individual channels $\boldsymbol{h}$ and $\boldsymbol{g}$ identifiable without ambiguity. If superimposed training is not employed, an N-dimensional binary search would be needed in order to estimate the vectors $\boldsymbol{h}$ and $\boldsymbol{g}$ up to a sign ambiguity [5].

$\mathcal{CCN}(0, P_2\boldsymbol{I}_N)$. In Section 5, we will examine the effect of this approximation using simulations. As we will see, the proposed semi-blind estimator performs well even when the data symbol vectors are drawn from discrete constellations such as QPSK.

Under the Gaussian assumption, the joint likelihood can be expressed in terms of the first and second order statistics of the vectors $\boldsymbol{y}, \boldsymbol{z}_1, \ldots, \boldsymbol{z}_K$. Let us denote by $\boldsymbol{\mu}$ and $\boldsymbol{C}$ the mean and covariance matrix of $\boldsymbol{y}$, respectively. From (4), we see that

$$\boldsymbol{\mu} = \mathbb{E}\{\boldsymbol{z}\} = A_p\boldsymbol{H}\boldsymbol{H}\boldsymbol{t}_1 + A_p\boldsymbol{H}\boldsymbol{G}\boldsymbol{t}_2 + \boldsymbol{H}\boldsymbol{t}_3, \tag{6}$$

$$\boldsymbol{C} = A_p^2\sigma^2\boldsymbol{H}\boldsymbol{H}^H + \sigma^2\boldsymbol{I}_N. \tag{7}$$

Furthermore, let us denote by $\boldsymbol{\mu}_k$ the mean of $\boldsymbol{z}_k$ and by $\boldsymbol{Q}$ the corresponding covariance matrix. It follows from (5) that

$$\boldsymbol{\mu}_k = \mathbb{E}\{\boldsymbol{z}_k\} = A_d\boldsymbol{H}\boldsymbol{H}\boldsymbol{s}_{1k}, \tag{8}$$

$$\boldsymbol{Q} = A_d^2P_2\boldsymbol{H}\boldsymbol{G}\boldsymbol{G}^H\boldsymbol{H}^H + A_d^2\sigma^2\boldsymbol{H}\boldsymbol{H}^H + \sigma^2\boldsymbol{I}_N. \tag{9}$$

Letting $\bar{\boldsymbol{z}} \triangleq [\boldsymbol{z}_1^T, \ldots, \boldsymbol{z}_K^T]^T$, the joint likelihood function of $\boldsymbol{y}$ and $\bar{\boldsymbol{z}}$ is given by[3]

$$f(\boldsymbol{y}, \bar{\boldsymbol{z}}; \boldsymbol{\theta}) = \frac{1}{\pi^N|\boldsymbol{C}|}e^{-(\boldsymbol{y}-\boldsymbol{\mu})^H\boldsymbol{C}^{-1}(\boldsymbol{y}-\boldsymbol{\mu})} \times \prod_{k=1}^{K}\frac{1}{\pi^N|\boldsymbol{Q}|}e^{-(\boldsymbol{z}_k-\boldsymbol{\mu}_k)^H\boldsymbol{Q}^{-1}(\boldsymbol{z}_k-\boldsymbol{\mu}_k)}. \tag{10}$$

Hence, the corresponding joint log-likelihood function is

$$\mathcal{L}(\boldsymbol{y}, \bar{\boldsymbol{z}}; \boldsymbol{\theta}) = -(K+1)N\log\pi - \log|\boldsymbol{C}| - K\log|\boldsymbol{Q}| - (\boldsymbol{y}-\boldsymbol{\mu})^H\boldsymbol{C}^{-1}(\boldsymbol{y}-\boldsymbol{\mu}) - \sum_{k=1}^{K}(\boldsymbol{z}_k-\boldsymbol{\mu}_k)^H\boldsymbol{Q}^{-1}(\boldsymbol{z}_k-\boldsymbol{\mu}_k). \tag{11}$$

Therefore, the semi-blind maximum-likelihood (ML) estimates of $\boldsymbol{h}$ and $\boldsymbol{g}$ are given by

$$\{\hat{\boldsymbol{h}}^{(s)}, \hat{\boldsymbol{g}}^{(s)}\} = \arg\min_{\boldsymbol{h},\,\boldsymbol{g}} \log|\boldsymbol{C}| + K\log|\boldsymbol{Q}| + (\boldsymbol{y}-\boldsymbol{\mu})^H\boldsymbol{C}^{-1}(\boldsymbol{y}-\boldsymbol{\mu}) + \sum_{k=1}^{K}(\boldsymbol{z}_k-\boldsymbol{\mu}_k)^H\boldsymbol{Q}^{-1}(\boldsymbol{z}_k-\boldsymbol{\mu}_k). \tag{12}$$

The solution to the minimization problem in (12) may be obtained using standard numerical techniques such as Newton or Quasi-Newton methods [13, 14]. In our work, we use the Broyden-Fletcher-Goldfarb-Shanno (BFGS) method. This is an efficient, low-complexity Quasi-Newton method which avoids the computation of the Hessian matrix and requires no matrix inversion. To initialize the BFGS algorithm, we can use the estimates provided by the low-complexity pilot-based LS estimator of [7].

4. CRAMER-RAO BOUND

In this section, we will derive the CRB for semi-blind estimation of the channel parameters $\boldsymbol{h}$ and $\boldsymbol{g}$. The CRB is obtained by treating the data as Gaussian-distributed. The joint log-likelihood in (11) may be expressed as $\mathcal{L}(\boldsymbol{y}, \bar{\boldsymbol{z}}; \boldsymbol{\theta}) = \mathcal{L}(\boldsymbol{y}; \boldsymbol{\theta}) + \mathcal{L}(\bar{\boldsymbol{z}}; \boldsymbol{\theta})$, where

$$\mathcal{L}(\boldsymbol{y}; \boldsymbol{\theta}) = -N\log\pi - \log|\boldsymbol{C}| - (\boldsymbol{y}-\boldsymbol{\mu})^H\boldsymbol{C}^{-1}(\boldsymbol{y}-\boldsymbol{\mu}) \tag{13}$$

is the log-likelihood for the pilot-bearing received vector and

$$\mathcal{L}(\bar{\boldsymbol{z}}; \boldsymbol{\theta}) = -K\log|\boldsymbol{Q}| - \sum_{k=1}^{K}(\boldsymbol{z}_k-\boldsymbol{\mu}_k)^H\boldsymbol{Q}^{-1}(\boldsymbol{z}_k-\boldsymbol{\mu}_k) \tag{14}$$

is the log-likelihood for the K information-bearing received vectors. The Fisher information matrix (FIM) for semi-blind estimation is thus given by

$$\boldsymbol{\Gamma}_s = \mathbb{E}\left\{\frac{\partial\mathcal{L}(\boldsymbol{y}, \bar{\boldsymbol{z}}; \boldsymbol{\theta})}{\partial\boldsymbol{\theta}^*}\frac{\partial\mathcal{L}(\boldsymbol{y}, \bar{\boldsymbol{z}}; \boldsymbol{\theta})}{\partial\boldsymbol{\theta}^T}\right\} = \boldsymbol{\Gamma}_p + \boldsymbol{\Gamma}_d, \tag{15}$$

where

$$\boldsymbol{\Gamma}_p = \mathbb{E}\left\{\frac{\partial\mathcal{L}(\boldsymbol{y}; \boldsymbol{\theta})}{\partial\boldsymbol{\theta}^*}\frac{\partial\mathcal{L}(\boldsymbol{y}; \boldsymbol{\theta})}{\partial\boldsymbol{\theta}^T}\right\} \tag{16}$$

is the FIM for pilot-based estimation and

$$\boldsymbol{\Gamma}_d = \mathbb{E}\left\{\frac{\partial\mathcal{L}(\bar{\boldsymbol{z}}; \boldsymbol{\theta})}{\partial\boldsymbol{\theta}^*}\frac{\partial\mathcal{L}(\bar{\boldsymbol{z}}; \boldsymbol{\theta})}{\partial\boldsymbol{\theta}^T}\right\} \tag{17}$$

is the FIM corresponding to the received data samples $\boldsymbol{z}_1, \ldots, \boldsymbol{z}_K$.

The FIM for the pilot-based channel estimation without superimposed training was obtained in [15], and it can be easily modified to obtain $\boldsymbol{\Gamma}_p$ by accounting for the presence of the superimposed pilot. In particular, we have that $\boldsymbol{\Gamma}_p = \boldsymbol{\Lambda}_p + \boldsymbol{\Sigma}_p$ where

$$\boldsymbol{\Lambda}_p = \begin{bmatrix} \frac{\partial\boldsymbol{\mu}^H}{\partial\boldsymbol{h}^*}\boldsymbol{C}^{-1}\frac{\partial\boldsymbol{\mu}}{\partial\boldsymbol{h}^T} & \frac{\partial\boldsymbol{\mu}^H}{\partial\boldsymbol{h}^*}\boldsymbol{C}^{-1}\frac{\partial\boldsymbol{\mu}}{\partial\boldsymbol{g}^T} \\ \frac{\partial\boldsymbol{\mu}^H}{\partial\boldsymbol{g}^*}\boldsymbol{C}^{-1}\frac{\partial\boldsymbol{\mu}}{\partial\boldsymbol{h}^T} & \frac{\partial\boldsymbol{\mu}^H}{\partial\boldsymbol{g}^*}\boldsymbol{C}^{-1}\frac{\partial\boldsymbol{\mu}}{\partial\boldsymbol{g}^T} \end{bmatrix}, \tag{18}$$

$$[\boldsymbol{\Sigma}]_{ij} = \mathrm{tr}\left(\boldsymbol{C}^{-1}\frac{\partial\boldsymbol{C}}{\partial\theta_i^*}\boldsymbol{C}^{-1}\frac{\partial\boldsymbol{C}}{\partial\theta_j}\right), \tag{19}$$

and

$$\frac{\partial\boldsymbol{\mu}}{\boldsymbol{h}^T} = 2A_p\boldsymbol{H}\boldsymbol{\Upsilon}(\boldsymbol{t}_1) + A\boldsymbol{G}\boldsymbol{\Upsilon}(\boldsymbol{t}_2) + \boldsymbol{\Upsilon}(\boldsymbol{t}_3),\ \frac{\partial\boldsymbol{\mu}}{\boldsymbol{g}^T} = \boldsymbol{0}_{N\times J}, \tag{20}$$

where $\boldsymbol{\Upsilon}(\boldsymbol{x})$ is the $N \times L$ circulant matrix with first column $\boldsymbol{x}$. The elements of $\boldsymbol{\Sigma}_p$ can be evaluated by noting that $\frac{\partial\boldsymbol{C}}{\partial h_i} = A_p^2\sigma^2\boldsymbol{E}_i\boldsymbol{H}^H$ and $\frac{\partial\boldsymbol{C}}{\partial g_i} = \boldsymbol{0}_{N\times N}$, where $\boldsymbol{E}_i$ is the $N \times N$ circulant matrix with first column[4] $\boldsymbol{e}_i$. The CRB for pilot-based estimation is thus given by $CRB_{\boldsymbol{\theta}}^{(p)} = \mathrm{tr}(\boldsymbol{\Gamma}_p^{-1})$.

We next find $\boldsymbol{\Gamma}_d$. From (14) we see that $\boldsymbol{\Gamma}_d = \sum_{k=1}^{K}\boldsymbol{\Gamma}_d^{(k)} + K\boldsymbol{\Sigma}_d$, where

$$\boldsymbol{\Gamma}_d^{(k)} = \begin{bmatrix} \frac{\partial\boldsymbol{\mu}_k^H}{\partial\boldsymbol{h}^*}\boldsymbol{Q}^{-1}\frac{\partial\boldsymbol{\mu}_k}{\partial\boldsymbol{h}^T} & \frac{\partial\boldsymbol{\mu}_k^H}{\partial\boldsymbol{h}^*}\boldsymbol{Q}^{-1}\frac{\partial\boldsymbol{\mu}_k}{\partial\boldsymbol{g}^T} \\ \frac{\partial\boldsymbol{\mu}_k^H}{\partial\boldsymbol{g}^*}\boldsymbol{Q}^{-1}\frac{\partial\boldsymbol{\mu}_k}{\partial\boldsymbol{h}^T} & \frac{\partial\boldsymbol{\mu}_k^H}{\partial\boldsymbol{g}^*}\boldsymbol{Q}^{-1}\frac{\partial\boldsymbol{\mu}_k}{\partial\boldsymbol{g}^T} \end{bmatrix}, \tag{21}$$

and

$$[\boldsymbol{\Sigma}_d]_{ij} = \mathrm{tr}\left(\boldsymbol{Q}^{-1}\frac{\partial\boldsymbol{Q}}{\partial\theta_i^*}\boldsymbol{Q}^{-1}\frac{\partial\boldsymbol{Q}}{\partial\theta_j}\right). \tag{22}$$

Since $\boldsymbol{\mu}_k = A_d\boldsymbol{H}\boldsymbol{H}\boldsymbol{s}_{1k}$, we have that

$$\frac{\partial\boldsymbol{\mu}_k}{\partial\boldsymbol{h}^T} = 2A_d\boldsymbol{H}\boldsymbol{\Upsilon}(\boldsymbol{s}_{1k}),\ \frac{\partial\boldsymbol{\mu}_k}{\partial\boldsymbol{g}^T} = \boldsymbol{0}_{N\times N}. \tag{23}$$

To evaluate (22), we can use the expression for $\boldsymbol{Q}$ in (9) to obtain

$$\frac{\partial\boldsymbol{Q}}{\partial h_i} = A_d^2P_2\boldsymbol{E}_i\boldsymbol{G}\boldsymbol{G}^H\boldsymbol{H}^H + A_d^2\sigma^2\boldsymbol{E}_i\boldsymbol{H}^H, \tag{24}$$

and

$$\frac{\partial\boldsymbol{Q}}{\partial g_i} = A_d^2P_2\boldsymbol{H}\boldsymbol{E}_i\boldsymbol{G}^H\boldsymbol{H}^H. \tag{25}$$

Finally, the semi-blind CRB is given by $CRB_{\boldsymbol{\theta}}^{(s)} = \mathrm{tr}(\boldsymbol{\Gamma}_s^{-1})$.

[3] $|\boldsymbol{A}|$ denotes the determinant of $\boldsymbol{A}$.

[4] The vector $\boldsymbol{e}_i$ is the $N \times 1$ basis vector with the ith element 1 and the remaining elements 0.

5. SIMULATION RESULTS

In this section, we investigate through simulations the performance of the proposed semi-blind algorithm and compare it to that of the fully pilot-based approach. Our results are obtained assuming that $P_1 = P_2 = \frac{1}{2}P_r$. In addition, we assume that $\boldsymbol{h}$ has 5 taps and $\boldsymbol{g}$ has 4. We average our results over a set of 100 independent realizations of $\boldsymbol{h}$ and $\boldsymbol{g}$. The taps of each channel vector are modelled as i.i.d. $\mathcal{CCN}(0,1)$. The number of carriers is set as $N = 64$. Unless mentioned otherwise, the number of data blocks is $K = 20$. The BFGS algorithm is employed to solve the minimization problem in (12), in combination with backtracking linesearch [13] that is used to find the appropriate step size at each iteration. We assume that the BFGS algorithm has converged when $\|\nabla\mathcal{L}(\bar{\boldsymbol{y}};\boldsymbol{\theta}^{\{n\}})\|^2 < 10^{-4}$, where $\boldsymbol{\theta}^{\{n\}}$ is the value of estimate of $\boldsymbol{\theta}$ at the nth iteration. To initialize the BFGS algorithm, we use the estimates provided by the pilot-based LS estimator derived in [7] followed by 3 iterations of the iterative improvement procedure proposed therein. The parameter α that controls power allocation for the superimposed pilot is fixed at 0.2. For comparison purposes, we consider the pilot-based LS estimator followed by 15 iterations of the iterative improvement procedure in [7].

In Fig. 2, we plot the MSE performances of the semi-blind algorithm and the pilot-based algorithm versus SNR along with the corresponding semi-blind and pilot-based CRBs. The MSE performance of the semi-blind estimator is shown for the case where the symbol vectors $\tilde{\boldsymbol{s}}_{1k}, \tilde{\boldsymbol{s}}_{2k}, k = 1,\ldots,K$ are $\mathcal{CCN}(0, P_2\boldsymbol{I}_N)$ as well as the case where they are generated using QPSK modulation. In both cases, as we can see from Fig. 2, the semi-blind approach provides a substantial improvement in accuracy over the pilot-based approach. Furthermore, the MSE of the semi-blind algorithm closely approaches the semi-blind CRB as SNR increases.

In Fig. 3 we show the average number of iterations needed for the BFGS algorithm to converge at different SNR values for Gaussian data. The average number of iterations drops below 24 at 12dB and below 10 at 21dB. Hence, the performance improvement provided by the semi-blind approach comes at a reasonable computational load.

Finally, in Fig. 4, we plot the MSE performance of the semi-blind algorithm versus the number of OFDM data blocks K, along with the semi-blind CRB for Gaussian data. As expected the accuracy of the semi-blind estimator improves as K increases, which shows that the longer the coherence time of the channel the more attractive the semi-blind approach becomes.

6. CONCLUSIONS

In this paper, we investigated semi-blind estimation of individual channels for OFDM-based AF TWRNs and compared it to the conventional pilot-based approach. To assist in the estimation of the individual channels, we employed superimposed training at the relay. The semi-blind ML estimator was implemented iteratively using the BFGS algorithm. As a performance benchmark, we derived the semi-blind CRB. Using simulation studies, we showed that the proposed semi-blind algorithm provides a substantial improvement in accuracy over the pilot-based approach. Moreover, the performance of the semi-blind algorithm closely approaches the derived semi-blind CRB. These performance gains come at a reasonable computational cost and do not require the channel to be constant for a long duration, which clearly establishes the merit and practicality of semi-blind channel estimation for AF TWRNs.

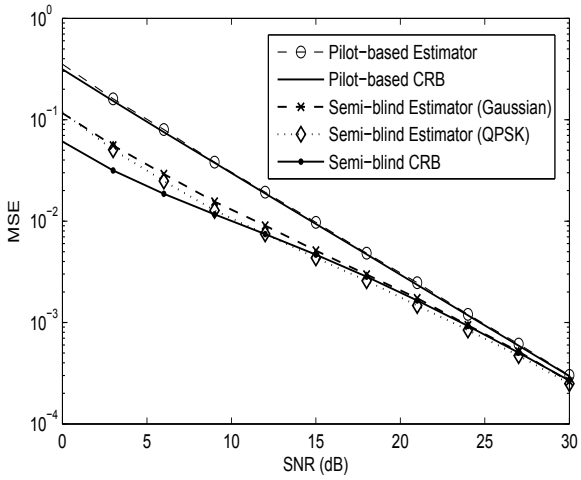

Fig. 2. MSE of the semi-blind and pilot-based algorithms along with the corresponding CRBs plotted versus SNR.

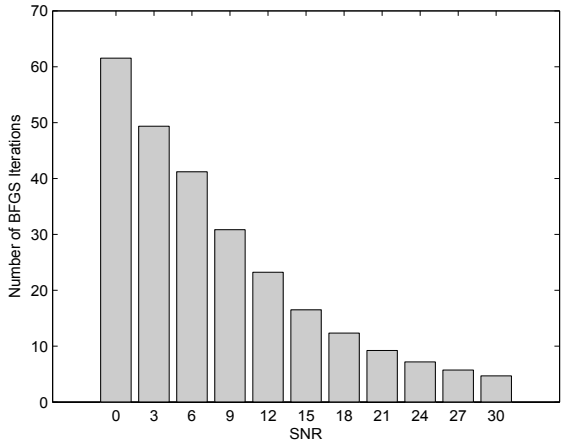

Fig. 3. Average number of iterations for the convergence of the BFGS algorithm at different SNR values.

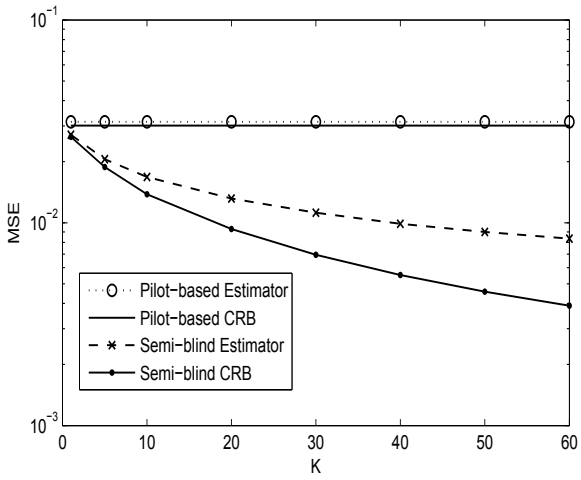

Fig. 4. MSE of the semi-blind algorithm CRBs plotted versus K. As reference we show the MSE and CRB of the pilot-based estimator.

7. REFERENCES

[1] B. Rankov and A. Wittneben, "Spectral efficient protocols for half-duplex fading relay channels," *IEEE J. Sel. Areas Commun.*, vol. 25, no. 2, pp. 379–389, Feb. 2007.

[2] S. Abdallah and I. N. Psaromiligkos, "Blind channel estimation for amplify-and-forward two-way relay networks employing M-PSK modulation," *IEEE Trans. Signal Process.*, vol. 60, no. 7, pp. 3604–3615, Jul. 2012.

[3] F. Gao, R. Zhang, and Y. Liang, "Optimal channel estimation and training design for two-way relay networks," *IEEE Trans. Commun.*, vol. 57, no. 10, pp. 3024–3033, Oct. 2009.

[4] F. Roemer and M. Haardt, "Tensor-based channel estimation (TENCE) and iterative refinements for two-way relaying with multiple antennas and spatial reuse," *IEEE Trans. Signal Process.*, vol. 58, no. 11, pp. 5720–5735, Nov. 2010.

[5] F. Gao, R. Zhang, and Y. Liang, "Channel estimation for OFDM modulated two-way relay networks," *IEEE Trans. Signal Process.*, vol. 57, no. 11, pp. 4443–4455, Nov. 2009.

[6] G. Wang, F. Gao, Y. C. Wu, and C. Tellambura, "Joint CFO and channel estimation for OFDM-based two-way relay networks," *IEEE Trans. Wireless Commun.*, vol. 10, no. 2, pp. 456–465, Feb. 2011.

[7] G. Wang, F. Gao, Z. X., and C. Tellambura, "Superimposed training-based joint CFO and channel estimation for CP-OFDM modulated two-way relay networks," *EURASIP J. Wireless Comm. and Network.*, vol. 2010, p. 9, 2010, ID=403936.

[8] X. Liao, L. F. Fan, and F. Gao, "Blind channel estimation for OFDM modulated two-way relay network," in *Proc. 12th IEEE Wireless Comm. and Networking Conf. (WCNC)*, Sydney, Australia, Apr. 2010.

[9] S. Abdallah and I. N. Psaromiligkos, "Exact Cramer-Rao bounds for semi-blind channel estimation in amplify-and-forward two-way relay networks employing square QAM modulation," *ArXiv pre-print cs.IT/1207.5483*, Jul. 2012.

[10] T.-H. Pham, Y.-C. Liang, H. Garg, and A. Nallanathan, "Joint channel estimation and data detection for MIMO-OFDM two-way relay networks," in *Proc. IEEE Global Comm. Conf. (Globecom)*, Miami, Florida, Dec. 2010.

[11] K. Lee, H. Sung, E. Park, and I. Lee, "Joint optimization for one and two-way mimo af multiple-relay systems," *IEEE Trans. Wireless Commun.*, vol. 9, no. 12, pp. 3671–3681, Dec. 2010.

[12] G. Wang, F. Gao, and C. Tellambura, "Superimposed pilot based joint CFO and channel estimation for CP-OFDM modulated two-way relay networks," in *Proc. IEEE Global Comm. Conf. (Globecom)*, Miami, Florida, Dec. 2010.

[13] S. Boyd and L. Vandenberghe, *Convex Optimization*. Cambridge, UK: Cambridge Univ. Pr., 2004.

[14] J. Nocedal and S. Wright, *Numerical Optimization*. Berlin, Germany: Springer-Verlag, 1999.

[15] S. Zhang, F. Gao, and C. Pei, "Optimal training design for individual channel estimation in two-way relay networks," *IEEE Trans. Signal Process.*, vol. 60, no. 9, pp. 4987–4991, 2012.